Diffusion in the random gap model of monolayer and bilayer graphene

K. Ziegler

Institut für Physik, Universität Augsburg, D-86135 Augsburg, Germany

In this paper we study the effect of a fluctuating gap in mono- and bilayer graphene, created by a symmetry-breaking random potential. We identify a continuous symmetry for the two-particle Green's function which is spontaneously broken in the average two-particle Green's function and leads to a massless fermion mode. Within a loop expansion it is shown that the massless mode is dominated on large scales by small loops. This result indicates diffusion of electrons. Although the diffusion mechanism is the same in mono- and in bilayer graphene, the amount of scattering is much stronger in the latter. Physical quantities at the neutrality point, such as the density of states, the diffusion coefficient, and the conductivity, are determined by the one-particle scattering rate. All these quantities vanish at a critical value of the average symmetry-breaking potential, signaling a continuous transition to an insulating behavior.

I. INTRODUCTION

Graphene is a single sheet of carbon atoms, where the latter form a honeycomb lattice. Graphene as well as a stack of two graphene sheets (i.e., a graphene bilayer) are semi-metals with remarkably good conducting properties.[1–3] These materials have been experimentally realized with external gates, which allow a continuous change in charge carriers. There exists a nonzero minimal conductivity at the charge neutrality point (NP). Its value is very robust and almost unaffected by disorder or thermal fluctuations.[3–6]

Many technological applications of graphene require an electronic gap to construct switching devices. A first step in this direction has been achieved by recent experiments with hydrogenated graphene[7] and gated bilayer graphene.[8–10] These experiments take advantage of the fact that the breaking of a discrete symmetry of the lattice system opens a gap in the electronic spectrum at the Fermi energy. A symmetry-breaking potential (SBP) is a staggered potential in the case of a monolayer, which breaks the sublattice symmetry of the honeycomb lattice, or a gate potential that distinguishes between the two layers in the case of bilayer graphene, where the latter breaks the symmetry between the layers. With this opportunity, one enters a new field, where one can switch between conducting and insulating regimes of a two-dimensional material, either by a chemical process (e.g., oxidation or hydrogenation) or by applying an external electric field.[11]

The opening of a *uniform* gap destroys the metallic state immediately. Thus the conductivity of the material would drop from a finite value of order e^2/h directly to zero. In a realistic system, however, the gap may not be uniform after turning on the SBP. This means that only locally the material becomes insulating, whereas in other regions of the sample it is still metallic. The situation can be compared with a classical random network of broken and unbroken bonds. The conductivity of such a network is nonzero as long as there is a percolating cluster of unbroken bonds. In such a system the transition from conducting to insulting behavior is presumably a second-order percolation transition.[12]

Disorder in mono- and bilayer graphene has been the subject of a number of recent numerical studies[13,14] and analytic calculations.[15–17] The results can be summarized by the statement that chiral-symmetry preserving disorder provides delocalized states whereas a chiral-symmetry breaking scalar potential disorder leads to Anderson localization, even at the NP. This breaks the chiral symmetry but still allows for delocalized states at the NP.[17,18] In contrast to chiral-symmetry preserving disorder, a random SBP reduces the minimal conductivity and can even lead to an insulating behavior.

In this paper an approach will be employed that eliminates a part of the complexity of the tight-binding model by focusing on continuous symmetries and corresponding spontaneous symmetry breaking. This allows us to identify a massless mode in the system with a randomly fluctuating SBP. Using a loop expansion we study the scaling behavior of the model and derive a diffusion propagator for the asymptotic behavior on large scales. Our result implies a relation between the average two-particle Green's function and the product two average one-particle Green's functions in self-consistent Born approximation. This is similar to the solution of the Bethe-Salpeter equation, a self-consistent equation for the average two-particle Green's function (Cooperon).[19–24] In addition to the latter we are also able to control the scaling behavior of all higher order terms in the loop expansion.

Our approach provides also information about the effect of symmetry-breaking terms. It turns out that the latter create a finite length scale $L_{\rm diff}$, such that diffusion breaks down for length scales L larger than $L_{\rm diff}$. Another reason for the breakdown of diffusion is a vanishing spontaneous symmetry breaking. This happens when the average value of the SBP exceeds a critical value. In this case there is no drop of the conductivity but a continuous decay to zero, depending on the fluctuations of the SBP.

This paper is organized as follows. In Sec. II the model and functional-integral representation of the Green's functions are introduced. The symmetries of the model are discussed in Sec. III. Then an effective functional integral is constructed for the average two-particle Green's function (Sec. IV) and a saddle-point approximation is employed (Sec. IV A). The invariance of the saddle-point equation of Sec. IV A under a continuous symmetry transformation requires the integration over a saddle-point manifold. This is

discussed in detail in Sec. V, which includes the loop expansion (Sec. V A). The results of the loop expansion and its consequences for the transport properties in graphene are discussed in Sec. VI. Finally, we conclude with a summary of our results in Sec. VII.

II. MODEL

Quasiparticles in monolayer graphene (MLG) or in bilayer graphene (BLG) are described in tight-binding approximation by a nearest-neighbor hopping Hamiltonian,

$$\mathbf{H} = -\sum_{\langle r,r'\rangle} t_{r,r'} c_r^\dagger c_{r'} + \sum_r V_r c_r^\dagger c_r + \text{H.c.}, \quad (1)$$

where $c_r^\dagger$ (c_r) are fermionic creation (annihilation) operators at lattice site r. The underlying lattice structure is either a honeycomb lattice (MLG) or two honeycomb lattices with Bernal stacking (BLG).[11,25] There is an intralayer hopping rate t and an interlayer hopping rate $t_\perp$ for BLG. V_r is either a staggered potential (MLG) with $V_r = m$ on sublattice A and $V_r = -m$ on sublattice B, or it is a biased gate potential in BLG that is $V_r = m$ ($V_r = -m$) on the upper (lower) graphene sheet. These potentials obviously break the sublattice symmetry of MLG and the symmetry between the two layers in BLG, respectively. A staggered potential can be the result of chemical absorption of other atoms in MLG (e.g., oxygen or hydrogen[7]). The potential in BLG has been realized as an external gate voltage, applied to the two layers of BLG.[8] A consequence of the symmetry breaking is the formation of a gap $\Delta_g = m$ in both systems: the spectrum of MLG consists of two bands with dispersion,

$$E_k = \pm \sqrt{m^2 + \epsilon_k^2}, \quad (2)$$

where

$$\epsilon_k^2 = t^2[3 + 2\cos k_1 + 4\cos(k_1/2)\cos(\sqrt{3}k_2/2)] \quad (3)$$

for lattice spacing $a = 1$. The spectrum of BLG consists of four bands[11] with two low-energy bands,

$$E_k^-(m) = \pm \sqrt{\epsilon_k^2 + t_\perp^2/2 + m^2 - \sqrt{t_\perp^4/4 + (t_\perp^2 + 4m^2)\epsilon_k^2}} \quad (4)$$

and two high-energy bands

$$E_k^+(m) = \pm \sqrt{\epsilon_k^2 + t_\perp^2/2 + m^2 + \sqrt{t_\perp^4/4 + (t_\perp^2 + 4m^2)\epsilon_k^2}}. \quad (5)$$

The spectrum of the low-energy bands has nodes for $m = 0$ where $E_k^-(0)$ vanishes. These nodes are the same as those of a single layer. For small gating potential we can expand $E_k^-(m)$ under the square root near the nodes and get

$$E_k^-(m) \sim \pm \sqrt{m^2 + E_k^-(0)^2}$$

with the same gap as in MLG.

The two bands in MLG and the two low-energy bands in BLG represent a spinor-1/2 wave function. This allows us to expand the corresponding Hamiltonian in terms of Pauli matrices σ_j as

$$H = h_1\sigma_1 + h_2\sigma_2 + m\sigma_3. \quad (6)$$

Near each nodes the coefficients h_j are[22]

$$h_j = i\nabla_j \text{(MLG)}, \quad h_1 = \nabla_1^2 - \nabla_2^2, \quad h_2 = 2\nabla_1\nabla_2 \text{(BLG)}, \quad (7)$$

where (∇_1, ∇_2) is the two-dimensional (2D) gradient.

Neither in MLG nor in BLG the potential is uniform. The reason in the case of MLG is that fluctuations appear in the coverage of the MLG by additional noncarbon atoms. In the case of BLG it is crucial that the graphene sheets are not planar but create ripples.[26–28] As a result, electrons experience a varying potential V_r along each graphene sheet, and m in the Hamiltonian of Eq. (6) is random variable in space. For BLG it is assumed that the gate voltage is adjusted at the NP such that in average m_r is exactly antisymmetric with respect to the two layers: $\langle m_1 \rangle_m = -\langle m_2 \rangle_m$.

At first glance, the Hamiltonian in Eq. (1) is a standard hopping Hamiltonian with random potential V_r. This is a model frequently used to study the generic case of Anderson localization.[29] The dispersion, however, is special in the case of graphene due to the honeycomb lattice: at low energies it consists of two nodes (or valleys) K and K'.[22,27] It is assumed here that weak disorder scatters only at small momentum such that intervalley scattering, which requires large momentum at least near the NP, is not relevant and can be treated as a perturbation. Then each valley contributes separately to transport, and the contribution of the two valleys to the conductivity σ is additive: $\sigma = \sigma_K + \sigma_{K'}$. This allows us to consider the low-energy Hamiltonian in Eqs. (6) and (7), even in the presence of randomness for each valley separately. Within this approximation the term m_r is a random variable with mean value $\langle m_r \rangle_m = \bar{m}$ and variance $\langle (m_r - \bar{m})(m_{r'} - \bar{m}) \rangle_m = g\,\delta_{r,r'}$. The following transport calculations will be based entirely on the Hamiltonian of Eqs. (6) and (7). In particular, the average Hamiltonian $\langle H \rangle_m$ can be diagonalized by Fourier transformation and is

$$\langle H \rangle_m = k_1\sigma_1 + k_2\sigma_2 + \bar{m}\sigma_3$$

for MLG with eigenvalues $E_k = \pm\sqrt{\bar{m}^2 + k^2}$. For BGL the average Hamiltonian is

$$\langle H \rangle_m = (k_1^2 - k_2^2)\sigma_1 + 2k_1k_2\sigma_2 + \bar{m}\sigma_3$$

with eigenvalues $E_k = \pm\sqrt{\bar{m}^2 + k^4}$.

Transport properties of the model can be calculated from the Kubo formula. Here we focus on interband scattering between states of energy $\omega/2$ and $-\omega/2$. This is related to the zitterbewegung,[30] which is a major contribution to transport near the NP. The frequency-dependent conductivity then reads[15]

$$\sigma_0(\omega) = -\frac{e^2}{2h}\omega^2\langle\langle\Phi_{-\omega/2}|r_k^2|\Phi_{\omega/2}\rangle\rangle_m, \quad (8)$$

where $|\Phi_E\rangle$ is the Fourier transform of the wave function under time evolution $\exp(-iHt)$,

$$|\Phi_E\rangle \equiv \int_0^\infty e^{(iE-\epsilon)t}|\Psi(t)\rangle dt = \int_0^\infty e^{(iE-\epsilon)t}e^{-iHt}dt|\Psi(0)\rangle$$

$$= -i(H - E - i\epsilon)^{-1}|\Psi(0)\rangle$$

$$= -iG(-E - i\epsilon)|\Psi(0)\rangle, \quad (9)$$

with the one-particle Green's function $G(z)=(H+z)^{-1}$. In other words, the conductivity is proportional to a matrix element of the position operator r_k ($k=1,2$) with respect to energy functions from the lower and the upper bands. The matrix element on the right-hand side is identical with the two-particle Green's function,

$$\langle\Phi_{-\omega/2}|r_k^2|\Phi_{\omega/2}\rangle = \sum_r r_k^2 \mathrm{Tr}_2[G_{r0}(-\omega/2-i\epsilon)G_{0r}(\omega/2+i\epsilon)].$$

With the identity $H=-\sigma_n H^T \sigma_n$, where $n=1$ for MLG and $n=2$ for BLG (cf. discussion in Sec. III), the matrix element also reads

$$\langle\Phi_{-\omega/2}|r_k^2|\Phi_{\omega/2}\rangle = -\sum_r r_k^2 \mathrm{Tr}_2[\sigma_n G_{r0}^T(\omega/2+i\epsilon)\sigma_n$$
$$\times G_{0r}(\omega/2+i\epsilon)]. \quad (10)$$

A. Functional integral

The two-particle Green's function on the right-hand side of Eq. (10) can be expressed, before averaging, as a Gaussian functional integral with two independent Gaussian fields, a boson (complex) field χ_{rk} and a fermion (Grassmann) field Ψ_{rk} ($k=1,2$) and their conjugate counterparts $\bar{\chi}_{rk}$ and $\bar{\Psi}_{rk}$,[31]

$$-G_{rr',jj'}^T(z)G_{r'r,k'k}(z) = \int \Psi_{r'j'}\bar{\Psi}_{rj}\chi_{rk}\bar{\chi}_{r'k'}$$
$$\times \exp[-S_0(z)]\mathcal{D}[\Psi]\mathcal{D}[\chi]. \quad (11)$$

$S_0(z)$ is a quadratic form of the four-component field $\phi_r = (\chi_{r1},\chi_{r1},\Psi_{r2},\Psi_{r2})$,

$$S_0(z) = -i\sum_{r,r'}\phi_r\cdot(\hat{H}+z)_{r,r'}\bar{\phi}_{r'} \quad (\mathrm{Im}\, z>0), \quad (12)$$

where the extended Hamiltonian $\hat{H}=\mathrm{diag}(H,H^T)$ of S_0 acts in the boson and in the fermion sector separately. The use of the mixed field ϕ_r has the advantage that an extra normalization factor for the integral is avoided. The matrix element in Eq. (10) reads now

$$\langle\Phi_{-\omega/2}|r_k^2|\Phi_{\omega/2}\rangle$$
$$= \sum_{j\neq k}\sum_r r_k^2[\langle\Psi_{0j}\bar{\Psi}_{rj}\chi_{rk}\bar{\chi}_{0k}\rangle_0 - (-1)^n\langle\Psi_{0j}\bar{\Psi}_{rk}\chi_{rj}\bar{\chi}_{0k}\rangle_0]$$
$$= -\sum_{j\neq k}\sum_r r_k^2[\langle\chi_{rk}\bar{\Psi}_{rj}\Psi_{0j}\bar{\chi}_{0k}\rangle_0 - (-1)^n\langle\chi_{rj}\bar{\Psi}_{rk}\Psi_{0j}\bar{\chi}_{0k}\rangle_0],$$
$$(13)$$

with

$$\langle\cdots\rangle_0 = \int \ldots \exp[-S_0(z)]\mathcal{D}[\Psi]\mathcal{D}[\chi].$$

III. SYMMETRIES

Transport properties are controlled by the symmetry of the Hamiltonian and of the corresponding one-particle Green's

function $G(i\epsilon)=(H+i\epsilon)^{-1}$. In the absence of sublattice-symmetry breaking (i.e., for $m=0$), the Hamiltonian $H = h_1\sigma_1+h_2\sigma_2$ has a continuous chiral symmetry

$$H \rightarrow e^{\alpha\sigma_3}He^{\alpha\sigma_3} = H \quad (14)$$

with a continuous parameter α, since H anticommutes with σ_3. The term $m\sigma_3$ breaks the continuous chiral symmetry. However, the behavior under transposition $h_j^T=-h_j$ for MLG and $h_j^T=h_j$ for BLG provides a discrete symmetry,

$$H \rightarrow -\sigma_n H^T \sigma_n = H, \quad (15)$$

where $n=1$ for MLG and $n=2$ for BLG. This symmetry is broken for the one-particle Green's function $G(i\epsilon)$ by the $i\epsilon$ term. To see whether or not the symmetry is restored for $\epsilon \rightarrow 0$, the difference of $G(i\epsilon)$ and the transformed Green's function $-\sigma_n G^T(i\epsilon)\sigma_n$ must be evaluated,

$$G(i\epsilon) + \sigma_n G^T(i\epsilon)\sigma_n = G(i\epsilon) - G(-i\epsilon). \quad (16)$$

For the diagonal elements this is the density of states at the NP $\rho(E=0)\equiv\rho_0$ in the limit $\epsilon\rightarrow 0$. Thus the order parameter for spontaneous symmetry breaking is ρ_0.

Equation (10) indicates that transport properties are expressed by the two-particle Green's function $G(i\epsilon)G(-i\epsilon)$. Each of the two Green's functions, $G(i\epsilon)$ and $G(-i\epsilon)$, can be considered as a random variable which are correlated due to the common random variable m_r. Their distribution is defined by a joint distribution function $P[G(i\epsilon),G(-i\epsilon)]$. In terms of transport theory, both the Green's functions must be included on equal footing. This is possible by introducing the extended Green's function,

$$\hat{G}(i\epsilon) = \begin{pmatrix} G(i\epsilon) & 0 \\ 0 & G(-i\epsilon) \end{pmatrix} = \begin{pmatrix} H+i\epsilon & 0 \\ 0 & H-i\epsilon \end{pmatrix}^{-1}. \quad (17)$$

In the present case one can use the symmetry transformation of H in Eq. (15) to write the extended Green's function as

$$\hat{G}(i\epsilon) = \begin{pmatrix} \sigma_0 & 0 \\ 0 & -\sigma_0 \end{pmatrix}\begin{pmatrix} \sigma_0 & 0 \\ 0 & i\sigma_n \end{pmatrix}$$
$$\times \begin{pmatrix} H+i\epsilon & 0 \\ 0 & H^T+i\epsilon \end{pmatrix}^{-1}\begin{pmatrix} \sigma_0 & 0 \\ 0 & i\sigma_n \end{pmatrix}.$$

The extended Hamiltonian $\hat{H}=\mathrm{diag}(H,H^T)$ is invariant under a global "rotation"

$$\hat{H} \rightarrow e^{\hat{S}}\hat{H}e^{\hat{S}} = \hat{H}, \quad \hat{S} = \begin{pmatrix} 0 & \alpha\sigma_n \\ \alpha'\sigma_n & 0 \end{pmatrix} \quad (18)$$

with continuous parameters α and α'. The invariance is a consequence of the fact that $\hat{H}$ anticommutes with S. The $i\epsilon$ term of the Green's function also breaks this symmetry. For $\alpha\alpha'=-\pi^2/4$ the diagonal element of $\hat{G}-e^S\hat{G}e^S$ is proportional to the density of states ρ_0. Thus, the continuous symmetry is spontaneously broken for $\epsilon\rightarrow 0$ if ρ_0 is nonzero. In this case there is a massless mode.

As a symmetry-breaking parameter, ϵ generates a characteristic response of the system with long-range correlations when it is varied for $\epsilon\sim 0$. This is reminiscent of a weak external magnetic field in a (classical) ferromagnet, where

the response to a change in the magnetic field creates a power-law magnetic susceptibility near the critical point. Moreover, if ϵ is chosen as a space-dependent field ϵ_r, we can vary it locally and obtain a space-dependent response in form of correlation functions of the Green's functions. This allows us to study complex correlation functions by taking local derivatives of the field ϵ_r.

Returning to the quadratic form in the action $S_0(z)$ of Eq. (12), we notice that after the rotation of the diag(H, H^T) with $e^{\hat{S}}$ off-diagonal block matrices are generated. These matrices should have Grassmann elements in order to have a quadratic form that has pairs of complex and pairs of Grassmann variables. Therefore, the parameters α and α' must be Grassmann variables: $\alpha = \psi$ and $\alpha' = \bar{\psi}$.

IV. AVERAGED MATRIX ELEMENTS

As an example, we need to consider the averaged matrix element of r_k^2 in Eq. (13). Averaging Eq. (11) over the Gaussian distribution of v_r means replacing $\exp(-S_0)$ by $\langle \exp(-S_0) \rangle_m$ on the right-hand side of the equation. The latter can be written again as an exponential function $\langle \exp(-S_0) \rangle_m = \exp(-S_1)$, where the new function S_1 contains also quartic terms of the field ϕ,

$$S_1 = -i \sum_{r,r'} \phi_r \cdot (H_0 + z)_{r,r'} \bar{\phi}_{r'} + g \sum_r (\phi_r \cdot \gamma_3 \bar{\phi}_r)^2. \quad (19)$$

Then it is convenient to transform the integration variables (Hubbard-Stratonovich transformation[31]) as

$$\begin{pmatrix} \chi_r \bar{\chi}_r & \chi_r \bar{\Psi}_r \\ \Psi_r \bar{\chi}_r & \Psi_r \bar{\Psi}_r \end{pmatrix} \rightarrow \hat{Q}_r = \begin{pmatrix} Q_r & \Theta_r \\ \bar{\Theta}_r & -iP_r \end{pmatrix}, \quad (20)$$

where Q_r and P_r are symmetric 2×2 matrices and Θ_r and $\bar{\Theta}_r$ are 2×2 matrices whose elements are independent Grassmann variables. Now the correlation functions in Eq. (13) can be rewritten as correlation functions in the new field $\hat{Q}_r$. Then the matrix element reads

$$\langle\langle \Phi_{-\omega/2} | r_k^2 | \Phi_{\omega/2} \rangle\rangle_m = -\frac{1}{g^2} \sum_{j \neq k} \sum_r r_k^2 [\langle (\Theta \sigma_3)_{r,jk} (\bar{\Theta} \sigma_3)_{0,kj} \rangle_2$$
$$- (-1)^n \langle (\Theta \sigma_3)_{r,jk} (\bar{\Theta} \sigma_3)_{0,jk} \rangle_2] \quad (21)$$

with

$$\langle \ldots \rangle_2 = \int \ldots \exp[-S_2(z)] \mathcal{D}\Psi \mathcal{D}[\hat{Q}]$$

and

$$S_2(z) = \sum_{r,r'} \frac{1}{g} \text{Trg}(\hat{Q}_r^2) + \ln[\det g(\langle \hat{H} \rangle_m + z - 2\gamma_3 \hat{Q})]. \quad (22)$$

Trg is the graded trace

$$\text{Trg}\left[\begin{pmatrix} A & \Theta \\ \bar{\Theta} & B \end{pmatrix}\right] = \text{Tr}\,A - \text{Tr}\,B,$$

Tr is the conventional trace, and detg is the graded determinant,[17]

$$\text{detg}\left(\begin{pmatrix} A & \Theta \\ \bar{\Theta} & B \end{pmatrix}\right) = \frac{\det(A)}{\det(B)} \det(\mathbf{1} - \bar{\Theta} B^{-1} \Theta A^{-1})$$

$$= \frac{\det(A - \bar{\Theta} B^{-1} \Theta)}{\det(B)}. \quad (23)$$

A. Saddle-point approximation

The integration in Eq. (21) can be performed in saddle-point approximation. The saddle point is obtained as the solution of $\delta S_2 = 0$. Assuming a solution of the form

$$\hat{Q}_0 = -i\frac{\eta}{2}\gamma_3 - \frac{m_s}{2}\gamma_0, \quad (24)$$

we obtain the parameters η and m_s from the saddle-point equation,

$$\hat{Q}_0 = g(\langle \hat{H} \rangle_m + z - 2\gamma_3 \hat{Q}_0)_{rr}^{-1} \gamma_3. \quad (25)$$

A consequence of the symmetry discussed in Sec. III is that for $z = 0$ the saddle-point equation is invariant under the global symmetry transformation $\hat{Q}_0 \rightarrow \hat{U}^{-1} \hat{Q}_0 \hat{U}$, where $\hat{U} = e^{\hat{S}}$ of Eq. (18). This transformation creates the saddle-point manifold

$$\hat{Q}_r' = -i\frac{\eta}{2}\gamma_3 \hat{U}_r^2 - \frac{m_s}{2}\gamma_0, \quad (26)$$

where $\hat{U}_r$ is obtained from Eq. (18) by replacing the transformation parameters α (α') by space-dependent Grassmann variables ψ_r ($\bar{\psi}_r$), respectively. The form of $\hat{Q}_r'$, which is dictated by the symmetry, implies for the action S_2 on the saddle-point manifold that (i) the quadratic term vanishes and (ii) the remaining term becomes

$$S' = \ln \text{detg}(\langle \hat{H} \rangle_m + m_s \sigma_3 + z + i\eta \hat{U}^2). \quad (27)$$

This action contains the symmetry-breaking field z. The matrix element of Eq. (21) becomes

$$\langle\langle \Phi_{-\omega/2} | r_k^2 | \Phi_{\omega/2} \rangle\rangle_m \approx \frac{4\eta^2}{g^2} \sum_r r_k^2 \langle \psi_r \bar{\psi}_0 \rangle_{S'}, \quad (28)$$

with

$$\langle \cdots \rangle_{S'} = \int \ldots e^{-S'} \mathcal{D}[\hat{U}] = \int \ldots e^{-S'} \mathcal{D}[\psi]. \quad (29)$$

There is no extra factor from the invariant integration measure when we replace $\mathcal{D}[\hat{U}]$ by $\mathcal{D}[\psi]$ (cf. Appendix A).

B. Evaluation of the scattering rate η

The saddle-point approximation of the average one-particle Green's function means

$$\langle G(z) \rangle_m = \langle (H + z)^{-1} \rangle_m \approx (\langle H \rangle_m + m_s \sigma_3 + z + i\eta)^{-1}$$
$$= G_0(z + i\eta), \quad (30)$$

which is often called self-consistent Born approximation.[19]

The ansatz for a uniform saddle-point solution in Eq. (24) leads to a shift of z as $z \to i\eta' \equiv i\eta + z$ with

$$\eta' + iz = \eta' gI \tag{31}$$

and a shift of the average mass $\bar{m} \to \bar{m} + m_s$ with

$$m_s = -\bar{m}gI/(1 + gI). \tag{32}$$

The integral I reads

$$I = 2 \int G_{0,11}(i\eta') d^2k/(2\pi)^2/(i\eta')$$

which is in the case of MLG

$$I \sim \frac{1}{\pi} \int_0^\lambda \left[\eta'^2 + (\bar{m} + m_s)^2 + k^2 \right]^{-1} k \, dk$$

$$= \frac{1}{2\pi} \ln\left[1 + \frac{\lambda^2}{\eta'^2 + (\bar{m} + m_s)^2} \right] \tag{33}$$

and in the case of BLG

$$I \sim \frac{1}{\pi} \int_0^\lambda (\eta'^2 + (\bar{m} + m_s)^2 + k^4)^{-1} k \, dk$$

$$= \frac{\arctan(\lambda^2/\sqrt{\eta'^2 + (\bar{m} + m_s)^2})}{2\pi\sqrt{\eta'^2 + (\bar{m} + m_s)^2}} \sim \frac{1}{4\sqrt{\eta'^2 + (\bar{m} + m_s)^2}} \tag{34}$$

for $\lambda \sim \infty$.

A nonzero solution η for $z = 0$ requires $gI = 1$ in Eq. (31), such that $m_s = -\bar{m}/2$ from Eq. (32). Since the integrals I are monotonically decreasing functions for large $\bar{m}$, a real solution with $gI = 1$ exists only for $|\bar{m}| \le m_c$. For both physical systems, MLG and BLG, the solutions read

$$\eta^2 = (m_c^2 - \bar{m}^2)\Theta(m_c^2 - \bar{m}^2)/4, \tag{35}$$

where the model dependence enters only through the critical average parameter m_c,

$$m_c = \begin{cases} \dfrac{2\lambda}{\sqrt{e^{2\pi/g} - 1}} \sim 2\lambda e^{-\pi/g} & \text{(MLG)} \\[2ex] g/2 & \text{(BLG)} \end{cases}. \tag{36}$$

m_c is much bigger for BGL, a result that indicates that the effect of disorder is much stronger in BLG. This is also reflected by the scattering rate at $\bar{m} = 0$ which is $\eta = m_c/2$.

V. INTEGRATION OVER THE SADDLE-POINT MANIFOLD

The integration weight $\exp(-S')$ of the functional integral in Eq. (29) reads according to Eq. (27),

$$\exp(-S') = \det g(H_0 + i\epsilon + i\eta \hat{U}^2)^{-1} \tag{37}$$

with the nonlinear field

$$\hat{U}^2 = e^{2\hat{S}} = \mathbf{1} + 2\hat{S} + 2\hat{S}^2$$

and $H_0 = \langle \hat{H} \rangle_m + m_s \sigma_3$. We notice that

$$\mathbf{1} + \hat{S} + \hat{S}^2 = (\mathbf{1} - \hat{S})^{-1},$$

since $\hat{S}^l = 0$ for $l \ge 3$. This enables us to rewrite the integration weight as

$$\exp(S') = \det g[H_0 + i\epsilon - i\eta + 2i\eta(\mathbf{1} - \hat{S})^{-1}]$$

$$= \det g[(\mathbf{1} - \hat{S})(H_0 + i\epsilon - i\eta) + 2i\eta] \det g(\mathbf{1} - \hat{S})^{-1}$$

$$= \det g[\mathbf{1} - \hat{S}(H_0 + i\epsilon - i\eta)(H_0 + i\epsilon + i\eta)^{-1}]$$

$$\times \det g(\mathbf{1} - \hat{S})^{-1}, \tag{38}$$

where we have used that $\det g(H_0 + i\epsilon + i\eta) = 1$. This result is remarkable because (i) $\hat{S}$ appears only linearly in the determinants and (ii) the matrix in the second determinant is diagonal,

$$\det g(1 - \hat{S}) = \prod_r (1 - 2\bar{\psi}_r \psi_r). \tag{39}$$

With the expression

$$\delta\hat{G}_0 := (H_0 + i\epsilon - i\eta)(H_0 + i\epsilon + i\eta)^{-1}$$

$$= \mathbf{1} - 2i\eta(H_0 + i\epsilon + i\eta)^{-1} \equiv \mathbf{1} - 2i\eta\hat{G}_0[i(\epsilon + \eta)],$$

we can write, using the definition of the graded determinant in Eq. (23),

$$\exp(-S') = \det g(\mathbf{1} - \hat{S}\delta\hat{G}_0)^{-1} \prod_r (1 - 2\bar{\psi}_r \psi_r)$$

$$= \det(\mathbf{1} - \bar{\psi}\sigma_1 \delta G_{0,11} \sigma_1 \psi \delta G_{0,22})^{-1} \prod_r (1 - 2\bar{\psi}_r \psi_r).$$

$\delta\hat{G}_0$ depends on ϵ and η and satisfies for $n = 1$ (MLG) or $n = 2$ (BLG),

$$\sigma_n \delta\hat{G}_{0,11}(\epsilon, \eta)\sigma_n = \sigma_n[\mathbf{1} - 2i\eta G_{0,11}(i\epsilon + i\eta)]\sigma_n$$

$$= \mathbf{1} + 2i\eta G_{0,22}(-i\epsilon - i\eta) = \delta\hat{G}_{0,22}(-\epsilon, -\eta).$$

This implies for the integration weight

$$\exp(-S') = \det(\mathbf{1} - \bar{\psi}h_-\psi h_+)^{-1} \prod_r (1 - 2\bar{\psi}_r \psi_r) \tag{40}$$

with $h_\pm = \delta G_{0,22}(\pm\epsilon, \pm\eta)$, whose Fourier components are

$$h_\pm \equiv \sigma_0 \mp 2i\eta G_{0,22}(\pm i\epsilon \pm i\eta)$$

$$= \sigma_0 \pm 2i\eta\sigma_n G_{0,11}(\mp i\epsilon \mp i\eta))\sigma_n$$

$$= \sigma_0 \mp \frac{2i\eta}{(\eta + \epsilon)^2 + h_1^2 + h_2^2}$$

$$\times [\mp i(\eta + \epsilon)\sigma_0 + (-1)^n(h_1\sigma_1 - h_2\sigma_2)]$$

$$= \left[1 - \frac{2\eta(\epsilon + \eta)}{(\eta + \epsilon)^2 + h_1^2 + h_2^2} \right]\sigma_0$$

$$\pm \frac{2i\eta(-1)^n}{(\eta + \epsilon)^2 + h_1^2 + h_2^2}(-h_1\sigma_1 + h_2\sigma_2). \tag{41}$$

Equation (40) is probably the most compact representation of $\exp(-S')$, and a corresponding simple visualization is
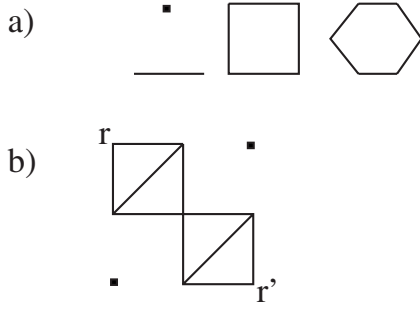
FIG. 1. (a) Elements of the loop expansion for the action S' and (b) for the two-particle Green's function $\langle G_{rr'}(z)G_{r'r}(-z)\rangle_m$. The dot corresponds with a simple factor $\psi_r\bar\psi_r$ from Eq. (39), whereas the loops with l corners correspond with the expansion term of order l in Eq. (42). Only an even number of corners can appear in the loop expansion (a) and each site must be visited twice by line elements in (b), except for the end points r and r', which are visited once.

that the lattice has isolated sites (due to $\bar\psi\psi\sigma_0$) or closed random walks of h_+ and h_- pairs (due to $\bar\psi h_-\psi h_+$). The functional integration in Eq. (29) can now be performed by expanding the determinant $\det(\mathbf{1}-\bar\psi h_-\psi h_+)^{-1}$ of Eq. (40) in powers of the Grassmann variables ψ_r and $\bar\psi_r$. A nonzero contribution to the integral requires that the entire lattice is covered with products $\psi_r\bar\psi_r$. This is quite different from the corresponding functional integral with respect to complex fields, where already a single term of the expansion gives a nonzero contribution. Consequently, the expansion must be organized in a specific way to control the integration over the Grassmann variables. This can be done in terms of a loop expansion of the action S' which is discussed in the next section.

A. Loop expansion

Starting from the expression in Eq. (40),

$$\det(\mathbf{1}-\bar\psi h_-\psi h_+)^{-1} = \exp[-\ln\det(\mathbf{1}-\bar\psi h_-\psi h_+)],$$

we can expand the exponent with trace terms of growing size as

$$\ln\det(\mathbf{1}-\bar\psi h_-\psi h_+) = -\sum_{l\geq 1}\frac{1}{l}Tr[(\bar\psi h_-\psi h_+)^l]$$
$$= \sum_{l\geq 1}\frac{1}{l}Tr[(h_-\psi h_+\bar\psi)^l]. \quad (42)$$

The trace terms can be visualized as closed polygons (loops) on the lattice with alternating ψ and $\bar\psi$ at the corners [cf. Fig. 1(a)], where each term is normalized by the number of corners of the loop l. Inserting this in the functional integral of Eq. (29), all the loops can contribute with the condition that they cover partially the lattice with products $\psi_r\bar\psi_r$. There are many graphically equivalent coverages (but with different values), as can be seen in Fig. 1(b): a square can either be a product of four $l=2$ contributions or just one $l=4$ contribution. This equivalence raises the question for the contribu-

tion(s) to a given graph with highest weight in the functional integral. A way to study this is a scaling analysis, where we analyze the change in the loop-expansion terms under a change in length scales. For this purpose it is convenient to choose the Fourier representation

$$Tr[(h_-\psi h_+\bar\psi)^l] = \int\ldots\int Tr_2[h_{-,k_1}\psi_{k_1-k_2}h_{+,k_2}\bar\psi_{k_2-k_3}$$
$$\cdots h_{-,k_{2l-1}}\psi_{k_{2l-1}-k_{2l}}h_{+,k_{2l}}\bar\psi_{k_{2l}-k_1}]d^2k_1\ldots d^2k_{2l}.$$

It should be noticed that there are only $2l-1$ integrations that affect the field ψ and its conjugate, namely $k_1-k_2, k_2-k_3,\ldots,k_{2l}-k_1$, since the sum of these variables gives zero. The integration over the remaining $2l^{th}$ variable affects only the h's. Using $\Delta_j=k_j-k_{j+1}$ with $k_{2l+1}=k_1$ we get

$$Tr[(h_-\psi h_+\bar\psi)^l] = \int C_{\Delta_1,\ldots,\Delta_{2l}}\psi_{\Delta_1}\bar\psi_{\Delta_2}\cdots\psi_{\Delta_{2l-1}}\bar\psi_{\Delta_{2l}}$$
$$\times\delta(\Delta_1+\ldots+\Delta_{2l})d^2\Delta_1\cdots d^2\Delta_{2l} \quad (43)$$

with the coefficient

$$C_{\Delta_1,\ldots,\Delta_{2l}} = \int Tr_2(h_{-,\Delta_1+\cdots+\Delta_{2l}+k_1}h_{+,\Delta_2+\cdots+\Delta_{2l}+k_1}$$
$$\cdots h_{-,\Delta_{2l-1}+\Delta_{2l}+k_1}h_{+,\Delta_{2l}+k_1})d^2k_1. \quad (44)$$

These integral expressions contribute with different weight to the loop expansion of $\exp(-S')$, depending on the number of corners l. In order to analyze the weights we can use the fact that Δ_j as well as ψ_{Δ_j} are integration variables in the functional integral. This enables us to rescale them as

$$\Delta_j\to s^{-1}\Delta_j, \quad \psi_{\Delta_j}\to s^{-\alpha}\psi_{s\Delta_j} \quad (45)$$

and use the integration symbols as before the rescaling. Then the scaling behavior of the general loop-expansion term in Eq. (43) is

$$\int C_{\Delta_1,\ldots,\Delta_{2l}}\psi_{\Delta_1}\bar\psi_{\Delta_2}\cdots\psi_{\Delta_{2l-1}}\bar\psi_{\Delta_{2l}}\delta(\Delta_1+\ldots+\Delta_{2l})$$
$$\times d^2\Delta_1\cdots d^2\Delta_{2l}\to s^{2l(2+\alpha)}s^{-2}\int C_{s\Delta_1,\ldots,s\Delta_{2l}}\psi_{\Delta_1}\bar\psi_{\Delta_2}$$
$$\cdots\psi_{\Delta_{2l-1}}\bar\psi_{\Delta_{2l}}\delta(\Delta_1+\ldots+\Delta_{2l})d^2\Delta_1\cdots d^2\Delta_{2l}. \quad (46)$$

Next, the contribution of $C_{s\Delta_1,\ldots,s\Delta_{2l}}$ to the prefactor must be determined. For $l=1$ we have $\Delta_2=-\Delta_1$ such that

$$\int Tr_2(h_{-,k_1}\psi_{k_1-k_2}h_{+,k_2}\bar\psi_{k_2-k_1})d^2k_1d^2k_2$$
$$= \int\psi_{\Delta_1}\int Tr_2(h_{-,k_1}h_{+,-\Delta_1+k_1})d^2k_1\bar\psi_{-\Delta_1}d^2\Delta_1$$
$$\equiv \int\psi_{\Delta_1}C_{\Delta_1}\bar\psi_{-\Delta_1}d^2\Delta_1. \quad (47)$$

This expression rescales as

$$\int \psi_k C_k \bar{\psi}_{-k} d^2k \to s^{2+2\alpha} \int \psi_k C_{sk} \bar{\psi}_{-k} d^2k,$$

where $C_{sk} \approx C_0 + s^2 k^2 C_0''$. Now we choose $\alpha = -2$ which gives a prefactor 1 for the $s^2 k^2 C_0''$ term.

In general, for $s < 1$ the rescaling of the wave vector in Eq. (45) has the effect that the integration is shifted to larger values in Δ_j (i.e., to shorter scales in real space). This is compensated by a prefactor in front of the integral. A prefactor smaller than 1 means that the integral contributes more on larger values of k_j than on smaller values. In other words, the corresponding loop contributes more to shorter length scales than to larger ones. Since we are interested in large-scale properties, terms with prefactors smaller than 1 are asymptotically irrelevant for this regime. The scaling of the coefficient

$$C_{s\Delta_1,\dots,s\Delta_{2l}} \sim \int \mathrm{Tr}_2(h_{-,s\Delta_1+\dots+s\Delta_{2l}+k_1} h_{+,s\Delta_2+\dots+s\Delta_{2l}+k_1}$$
$$\cdots h_{-,s\Delta_{2l-1}+s\Delta_{2l}+k_1} h_{+,s\Delta_{2l}+k_1}) d^2k_1$$

for $l \geq 2$ can be studied by rescaling $h_\pm$. Then we have for each factor $h_{\pm, s\Delta_j + \dots + \Delta_{2l} + k_1}$

$$h_{\pm, s\Delta_j + \dots \Delta_{2l} + k_1} = h_{\pm, k_1} + s(\Delta_j + \dots + \Delta_{2l}) h_{\pm, k_1}' + o(s^2).$$
(48)

such that

$$C_{s\Delta_1,\dots,s\Delta_{2l}} \sim C_0 + s \sum_{j_1=1}^{2l} C_{j_1} \Delta_{j_1} + \cdots$$
$$+ s^l \sum_{j_1,\dots,j_l=1}^{2l} C_{j_1,\dots,j_l} \prod_{n=1}^{l} \Delta_{j_n} + o(s^{2l+1}).$$

Here it is important to notice that each Δ_j becomes a gradient term in real space, whereas a constant term in Δ_j is diagonal in real space. Therefore, at least every second factor Δ_j (i.e., either Δ's with $j = 1, 3, \dots, 2l-1$ or $j = 2, 4, \dots, 2l$) must be present since otherwise multiple factors of ψ_r or $\bar{\psi}_r$ at the same site r would appear which gives zero due to the fact that these are Grassmann variables. Thus the leading behavior of the right-hand side of Eq. (46) under scaling is

$$\sim s^{2l(2+\alpha)} s^{l-2} \int C_{\Delta_1,\dots,\Delta_{2l}} \psi_{\Delta_1} \bar{\psi}_{\Delta_2} \cdots \psi_{\Delta_{2l-1}} \bar{\psi}_{\Delta_{2l}}$$
$$\times \delta(\Delta_1 + \dots + \Delta_{2l}) d^2\Delta_1 \cdots d^2\Delta_{2l}.$$

For $\alpha = -2$ this means that only terms with $l \leq 2$ are relevant for $s \sim 0$. Moreover, the $l = 2$ term vanishes since there are two contributions that cancel each other. This can easily be seen in real-space representation,

$$\mathrm{Tr}(h_- \psi h_+ \bar{\psi} h_- \psi h_+ \bar{\psi})$$
$$= \sum_{r_1,\dots,r_4} \mathrm{Tr}_2(h_{-,r_1-r_2} h_{+,r_2-r_3} h_{-,r_3-r_4} h_{+,r_4-r_1}) \psi_{r_2} \bar{\psi}_{r_3} \psi_{r_4} \bar{\psi}_{r_1}.$$

The leading nonvanishing term is of order s^2. In this case,

according to the gradient expansion, every second term is diagonal and reads,

$$\mathrm{Tr}_2(h_{-,0} h_{+,r_1-r_3} h_{-,0} h_{+,r_3-r_1}) \psi_{r_1} \bar{\psi}_{r_3} \psi_{r_3} \bar{\psi}_{r_1}$$
$$+ \mathrm{Tr}_2(h_{-,r_1-r_2} h_{+,0} h_{-,r_2-r_1} h_{+,0}) \psi_{r_2} \bar{\psi}_{r_2} \psi_{r_1} \bar{\psi}_{r_1}.$$

After renaming the summation indices and exchanging of the Grassmann factors in the first term we get

$$= [-\mathrm{Tr}_2(h_{-,0} h_{+,r_1-r_2} h_{-,0} h_{+,r_2-r_1})$$
$$+ \mathrm{Tr}_2(h_{-,r_1-r_2} h_{+,0} h_{-,r_2-r_1} h_{+,0})] \psi_{r_2} \bar{\psi}_{r_2} \psi_{r_1} \bar{\psi}_{r_1}.$$

Now we use the fact that $h_\pm = \kappa_0 \sigma_0 \pm (\kappa_1 \sigma_1 + \kappa_2 \sigma_2)$ in Eq. (41) and get from the sum of the two trace terms zero. This result implies that the loop expansion is asymptotically dominated by the term in Eq. (47) (i.e., the loop with two corners) which give the propagator

$$\sum_r e^{-iq \cdot r} \langle \psi_r \bar{\psi}_0 \rangle \sim \frac{1}{-2 + C_q}.$$
(49)

Here C_q can be expanded in powers of q (cf. Appendix B) as

$$C_q = 2 - \frac{4\eta^2}{g\eta'}(\epsilon + Dq^2) + o(q^3)$$

with the diffusion coefficient

$$D := -\frac{g\eta'}{2} \frac{\partial^2}{\partial q_k^2} \int \mathrm{Tr}_2[G_{0,22,k}(\epsilon + \eta) G_{0,22,k-q}(-\epsilon - \eta)] d^2k \big|_{q=0}.$$
(50)

Thus the propagator in Eq. (49) describes diffusion on large scales. The ϵ term corresponds with the symmetry-breaking parameter. The latter does not need to be a scalar but can be any symmetry-breaking tensor in the Green's function, provided it allows us to write the two-particle Green's function in the form of Eq. (17).

The matrix element of Eq. (28) reads with these expressions and the substitution $\epsilon \to i\omega/2$,

$$\langle\langle \Phi_{\omega/2} | r_k^2 | \Phi_{-\omega/2} \rangle\rangle_m = -\frac{\partial^2}{\partial q_k^2} \frac{\eta'}{g} \frac{1}{i\omega/2 + Dq^2} \bigg|_{q=0} = -8 \frac{\eta' D}{g\omega^2}.$$

We can also use the definition of D in Eq. (50), together with Eq. (10), to write

$$D = \frac{g\eta'}{2} \langle \Phi_{i\eta'}^0 | r_k^2 | \Phi_{-i\eta'}^0 \rangle$$
(51)

and

$$\langle\langle \Phi_{\omega/2} | r_k^2 | \Phi_{-\omega/2} \rangle\rangle_m = -\frac{\eta'^2}{(\omega/2)^2} \langle \Phi_{i\eta'}^0 | r_k^2 | \Phi_{-i\eta'}^0 \rangle,$$
(52)

where $|\Phi_E^0\rangle$ is the wave function of Eq. (9), when the Hamiltonian is replaced by the translational-invariant Hamiltonian H_0. Moreover, the integration in Eq. (50) gives for $\lambda \sim \infty$ (cf. Appendix C),

$$D = \frac{ag\eta'}{(4\eta'^2 + \bar{m}^2)\pi} \quad (a = 1 \text{ for MLG}, \quad a = 2 \text{ for BLG}),$$

$$\text{(53)}$$

which implies

$$\langle\langle\Phi_{\omega/2}|r_k^2|\Phi_{-\omega/2}\rangle\rangle_m \sim -\frac{8a\eta'^2}{\omega^2(4\eta'^2 + \bar{m}^2)\pi}. \quad \text{(54)}$$

VI. DISCUSSION

All our results are obtained for the charge neutrality point $E = 0$, for mono- and for bilayer graphene. The main results are given in Eqs. (49), (52), (51), and (53): Eq. (49) connects the average two-particle Green's function with the two-particle Green's function of the average Hamiltonian. A special consequence is Eq. (52), which describes a relation between a disorder-averaged matrix element and the corresponding matrix element of the pure system. Equation (51) connects the matrix element with the diffusion coefficient. And finally, Eq. (53) connects the diffusion coefficient with the one-particle scattering rate η.

Density of states. The average density of states is proportional to the diagonal element of the average one-particle Green's function $\langle(H + i\epsilon)^{-1}\rangle_m$. The latter can be evaluated in saddle-point approximation from Eq. (25) as

$$\langle G(i\epsilon)\rangle_m \approx G_0(i\epsilon + i\eta), \quad \text{(55)}$$

where the parameters η (scattering rate) and m_s are determined by the self-consistent (or saddle-point) conditions of Eqs. (31) and (32). We then obtain $\rho_0 \approx \eta/2\pi g$, where the scattering rate η is a function of g and $\bar{m}$, according to Eq. (35). The density of states has a semicircular form with respect to $\bar{m}$,

$$\rho_0 \approx \frac{\eta}{2\pi g} = \frac{1}{4\pi g}\sqrt{m_c^2 - \bar{m}^2}\,\Theta(m_c^2 - \bar{m}^2), \quad \text{(56)}$$

where the radius of the semicircle m_c is given in Eq. (36).

Diffusion. Scattering by the random gap term leads to diffusion, as explained in the loop expansion of Sec. V A. The diffusion coefficient D in Eq. (53) depends only on η'. This corresponds with the simple physical picture that diffusion decreases with an increasing scattering rate. Diffusion breaks down when the symmetry is broken by the parameter ϵ. This implies a maximal diffusion length $L_{\text{diff}} = \sqrt{2D/\epsilon}$. The scale L_{eff} indicates that any symmetry-breaking term creates a finite diffusion length which limits diffusion to systems of linear size L_{eff}. This length scale can be very large due to the large diffusion coefficient D in MLG,

$$L_{\text{diff}} \sim \frac{1}{2\sqrt{\pi}}\sqrt{\frac{ge^{\pi/g}}{\lambda\epsilon}}.$$

In the case of BLG, however, it is much smaller because of the stronger scattering rate $\eta = m_c/2$ of Eq. (36),

$$L_{\text{diff}} \sim \sqrt{\frac{2}{\pi\epsilon}}.$$

Matrix element. The averaged matrix element $\langle\langle\Phi_{\omega/2}|r_k^2|\Phi_{-\omega/2}\rangle\rangle_m$ is an indicator of Anderson localization since it diverges if the localization length is infinite. According to Eq. (54), the states $|\Phi_{\pm\omega/2}\rangle$ are delocalized at $\omega = 0$. On the other hand, the states are localized for $\omega \neq 0$ with a decreasing localization length as one goes away from the NP. Such a behavior was also found for bond disorder in analytic[15] and in numerical studies.[14]

Relation between averaged and nonaveraged Green's functions. In general, the average two-particle Green's function can be expressed by the function C_q through Eq. (49). C_q in Eq. (B2) is a function of the Green's functions $G_0(\pm\eta')$, where the random Hamiltonian $\hat{H}$ is replaced by the average Hamiltonian H_0. Since the average Hamiltonian is translational invariant, the function C_q can be easily calculated. This relation between the average two-particle Green's function and the self-consistent two-particle Green's function

$$\sum_r e^{-iq\cdot r}\text{Tr}_2[\langle G_{r0}(-i\epsilon)G_{0r}(i\epsilon)\rangle_m] \approx \frac{1}{-2 + C_q}$$

can be considered as a generalization of the self-consistent Born approximation of the one-particle Green's function in Eq. (55). Like in the latter case, the averaging process leads to a change in energies $\epsilon \to \eta'$ (i.e., a replacement of the symmetry-breaking parameter by the scattering rate). A consequence for the matrix element is Eq. (52), which means a simple scaling relation between the average matrix element and the matrix element of the average translational-invariant Hamiltonian H_0. [The scale η', however, is not free but fixed by the disorder average through the saddle-point Eq. (25).] This provides an interesting and useful relation between the averaged and the nonaveraged Green's functions. Moreover, in the relation of the matrix elements there is an extra prefactor $-\eta'^2/(\omega/2)^2$. This is important for the transport properties since it provides the delocalization of states at $\omega = 0$ and it cancels the factor ω^2 in the conductivity of Eq. (8). The relation in Eq. (52) can also be understood as a factorization of the averaged matrix element into a product of a power law (i.e., $\sim \omega^{-2}$) and a smooth scaling function $\eta'^2\langle\Phi_{i\eta'}^0|r_k^2|\Phi_{-i\eta'}^0\rangle$.

Conductivity. The conductivity of Eq. (8) is calculated from the matrix element in Eq. (54) and gives

$$\sigma_0(\omega) \sim \frac{4a\eta'^2}{\pi(4\eta'^2 + \bar{m}^2)}\Theta(m_c^2 - \bar{m}^2)\frac{e^2}{h}. \quad \text{(57)}$$

It is remarkable that η' drops out for $\bar{m} = 0$ which gives a frequency-independent result,

$$\sigma_0(\omega) \sim \frac{a}{\pi}\frac{e^2}{h}.$$

A frequency-independent conductivity was also found for a random vector potential.[15] In the absence of disorder a constant $\sigma(\omega)$ was found, with a different value though.[32,33] The difference is due the fact that the expression in Eq. (8) is only a contribution due to interband scattering from the total Kubo formula (for details cf. Ref. 15).
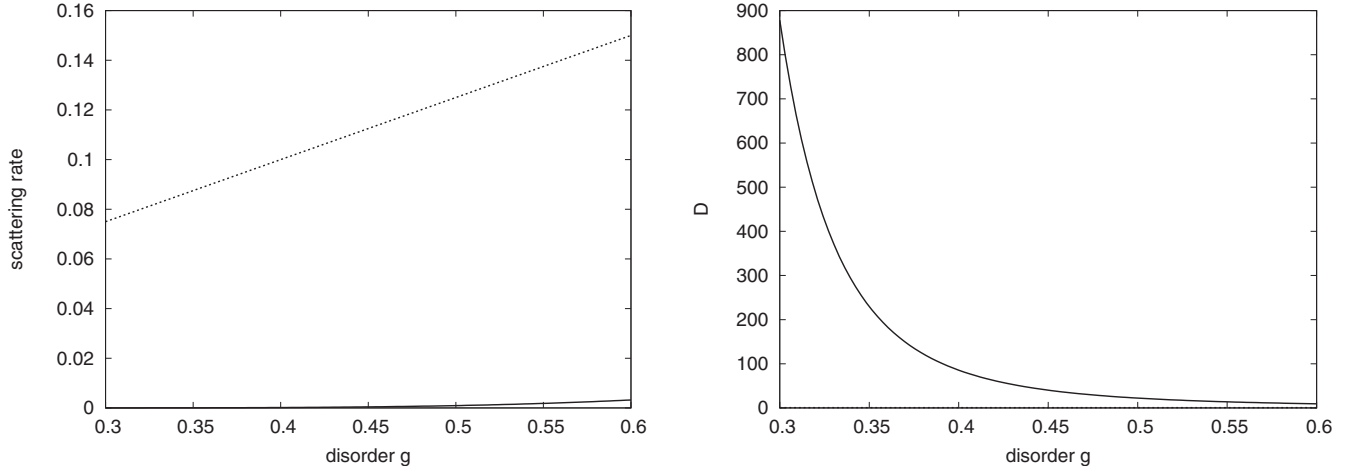
FIG. 2. Scattering rate η and diffusion coefficient D for $\bar{m}=0$ in the case of monolayer graphene (full curves) and bilayer graphene (dashed curves) versus the variance g of the random symmetry-breaking potential. The diffusion coefficient of bilayer graphene is so small ($D \sim 2/\pi$) such that it cannot be distinguished from the g axis.

dc conductivity. For $\omega \sim 0$ the parameter η' is replaced by the scattering rate η of Eq. (36). The resulting dc conductivity reads

$$\sigma_0(\omega \sim 0) \sim \frac{4a\eta^2}{\pi(4\eta^2 + \bar{m}^2)}\frac{e^2}{h} = \frac{a}{\pi}\left(1 - \frac{\bar{m}^2}{m_c^2}\right)\Theta(m_c^2 - \bar{m}^2)\frac{e^2}{h}. \tag{58}$$

Our knowledge of the diffusion coefficient D in Eq. (53) and the density of states ρ_0 in Eq. (56) allows us to evaluate the dc conductivity alternatively through the Einstein relation,

$$\sigma(\omega \sim 0) \propto \rho D \frac{e^2}{h} \approx \frac{a}{8\pi^2}\left(1 - \frac{\bar{m}^2}{m_c^2}\right)\Theta(m_c^2 - \bar{m}^2)\frac{e^2}{h}.$$

This agrees with Eq. (58), except for a constant factor.

It is important to notice that the conductivity at $\bar{m}=0$ does not depend on the variance g of the random SBP. This indicates that this quantity is robust against random fluctuations in graphene. In particular, we could have started from the action in Eq. (19) and treated the interaction term in perturbation theory in powers of g to obtain the same result. This idea was indeed employed in Ref. 16 and gave the same value for the minimal conductivity. However, it is not possible to obtain a nonzero critical value m_c in the case of MLG, since all orders of the expansion of m_c in Eq. (36) give zero. This is one of the reasons why we have not used the perturbation theory in g here but the loop expansion of Sec. V A.

VII. CONCLUSION

The physics of the random gap model is characterized by a discrete symmetry of the Hamiltonian and a continuous symmetry of the two-particle Green's function. For the disorder-averaged two-particle Green's function the continuous symmetry is represented by a fermionic degree of freedom. Since the symmetry is spontaneously broken, the resulting massless fermion mode controls the properties on large scales. An effective action is derived for the massless fermion mode and a loop expansion is employed to extract the dominant large-scale contribution. It is found that the shortest loops are in control of the large scales, leading to diffusion. An explicitly broken symmetry generates a finite diffusion length L_{diff} such that diffusion is possible only on length scales less than L_{diff}.

Although our models of mono- and bilayer graphene share the same type of symmetries and symmetry breaking, the quantitative properties are quite different since scattering is much stronger in bilayer graphene (cf. Fig. 2). For instance, the diffusion coefficient D is very large for monolayer graphene, namely,

$$D \propto g e^{\pi/g}$$

for average symmetry-breaking potential $\bar{m}=0$ because the low density of states at the neutrality point does not provide much scattering. This means that transport in monolayer graphene is practically ballistic if disorder is not too strong. In the case of bilayer graphene, however, scattering is much stronger because of a large density of states at the neutrality point, leading to a constant diffusion coefficient $D \sim 2/\pi$ for $\bar{m}=0$. This also implies a large diffusion length scale L_{diff} for monolayer graphene since $L_{\text{diff}} \propto \sqrt{D}$.

All physical quantities of our discussion (i.e., the average density of states, the diffusion coefficient, and the matrix element of the position operator) depend on the model parameters only through the one-particle scattering rate η. An exceptional case is the conductivity for vanishing average symmetry-breaking potential which is independent of the model parameters at all and has the value $e^2/\pi h$ for monolayer graphene and $2e^2/\pi h$ for bilayer graphene (up to a factor 4 for spin and valley degeneracy). This implies a frequency-independent microwave conductivity. On the other hand, an increasing average symmetry-breaking potential $\bar{m}$ reduces continuously the conductivity as well as the diffusion coefficient. The continuous behavior of the conductivity

with respect to gap opening is similar to a recent experimental observation by Adam *et al.*[34]

ACKNOWLEDGMENT

APPENDIX A: INTEGRATION OVER THE NONLINEAR FIELD

We consider the matrix expansion at fixed site r,

$$\hat{Q} = Q_{11} + Q_{12} + \cdots,$$

where $\{Q_{ij}\}$ is a basis for the matrix $\hat{Q}$. In the integral

$$I_1 = \int f(Q_{11,11}, Q_{12,12}, Q_{21,12}, \ldots),$$

$Q_{11,11}$ is replaced by the nonlinear term $Q_{11,11} + 1 + Q_{12,12}Q_{21,12}$ which is created by the diagonal matrix elements of $\hat{U}^2$ from the saddle-point manifold. This leads to the new integral

$$I_2 = \int f(Q_{11,11} + 1 + Q_{12,12}Q_{21,12}, Q_{12,12}, Q_{21,12}, \ldots).$$

An expansion in terms of the Grassmann variable $Q_{12,12}Q_{21,12}$ gives

$$I_2 = \int f(Q_{11,11} + 1, Q_{12,12}, Q_{21,12}, \ldots) \\ + \int Q_{12,12}Q_{21,12} f'(Q_{11,11} + 1, Q_{12,12}, Q_{21,12}, \ldots)$$

The second term vanishes at the $Q_{11,11}$ integration boundaries. Moreover, the shift in the first term by 1 can be removed, since the integration of $Q_{11,11}$ goes from $-\infty$ to ∞. This gives

$$I_2 = \int f(Q_{11,11}, Q_{12,12}, Q_{21,12}, \ldots) = I_1.$$

APPENDIX B: DIFFUSION PROPAGATOR

C_q is defined in Eq. (44),

$$C_q = \int \text{Tr}_2(h_{-,k}h_{+,k-q}) d^2k$$

$$= \int \text{Tr}_2[\sigma_0 - 2i\eta G_{0,22,k}(i\epsilon + i\eta)]$$

$$\times [\sigma_0 + 2i\eta G_{0,22,k-q}(-i\epsilon - i\eta)] d^2k$$

$$= \int \{2 + 2i\eta \text{Tr}_2[G_{0,22,k-q}(-i\epsilon - i\eta) - G_{0,22,k}(i\epsilon + i\eta)]$$

$$+ 4\eta^2 \text{Tr}_2[G_{0,22,k}(i\epsilon + i\eta)G_{0,22,k-q}(-i\epsilon - i\eta)]\} d^2k$$

$$= 2 + \int \{2i\eta \text{Tr}_2[G_{0,22,k-q}(-i\epsilon - i\eta) - G_{0,22,k}(i\epsilon + i\eta)]$$

$$+ 4\eta^2 \text{Tr}_2[G_{0,22,k}(i\epsilon + i\eta)G_{0,22,k-q}(-i\epsilon - i\eta)]\} d^2k, \tag{B1}$$

since the k integral is normalized. The Green's function reads

$$G_{0,22,k}(i\epsilon + i\eta) = -\frac{1}{(\epsilon + \eta)^2 + h_1^2 + h_2^2}[i(\epsilon + \eta) - h_1\sigma_1 + h_2\sigma_2].$$

Using the saddle-point Eq. (25) with $\eta' = \eta + \epsilon$, we have

$$\eta = \pm ig\text{Tr}_2[G_{0,22,rr}(\pm i\eta')].$$

This implies

$$\text{Tr}_2[G_{0,22,rr}(-i\eta') - G_{0,22,rr}(i\eta')] = 2i\eta/g,$$

such that

$$C_q = 2 - \frac{4\eta^2}{g} + 4\eta^2 \int \text{Tr}_2[G_{0,22,k}(i\eta')G_{0,22,k-q}(-i\eta')] d^2k. \tag{B2}$$

The second term can be expanded in powers of q,

$$C_q = 2 - \frac{4\eta^2}{g} + 4\eta^2 \int \text{Tr}_2[G_{0,22,k}(i\eta')G_{0,22,k}(-i\eta')] d^2k$$

$$+ 2\eta^2 q_k^2 \frac{\partial^2}{\partial q_k^2} \int \text{Tr}_2[G_{0,22,k}(i\eta')G_{0,22,k-q}(-i\eta')] d^2k|_{q=0}$$

$$+ o(q^3). \tag{B3}$$

Since G_0 satisfies the following relations:

$$G_0(i\eta')G_0(-i\eta') = (i\eta' + h_0)^{-1}(-i\eta' + h_0)^{-1} = (\eta'^2 + h_0^2)^{-1}$$

and

$$G_0(i\eta') - G_0(-i\eta') = (i\eta' + h_0)^{-1} - (-i\eta' + h_0)^{-1}$$
$$= -2i\eta'(\eta'^2 + h_0^2)^{-1},$$

we obtain

$$\text{Tr}_2 G_0(i\eta')G_0(-i\eta') = \frac{i}{2\eta'}\text{Tr}_2[G_0(i\eta') - G_0(-i\eta')].$$

This allows us to write for the third term in Eq. (B3),

$$4\eta^2 \int \text{Tr}_2[G_{0,22,k}(i\eta')G_{0,22,k}(-i\eta')] d^2k$$

$$= 4\eta^2 \text{Tr}_2[G_{0,22}(i\eta')G_{0,22}(-i\eta')]_{rr}$$

$$= 2i\frac{\eta^2}{\eta'}\text{Tr}_2[G_{0,22}(i\eta') - G_{0,22}(-i\eta')]_{rr} = 4\frac{\eta^3}{g\eta'}.$$

This gives

$$C_q = 2 - \frac{4\eta^2}{g\eta'}\left\{\epsilon - q_k^2\frac{g\eta'}{2}\frac{\partial^2}{\partial q_k^2}\int \mathrm{Tr}_2[G_{0,22,k}(i\eta')\right.$$

$$\left.\times G_{0,22,k-q}(-i\eta')]d^2k|_{q=0}\right\} + o(q^3).$$

Then the prefactor D of the q_k^2 term reads

$$D := -\frac{g\eta'}{2}\frac{\partial^2}{\partial q_k^2}\int \mathrm{Tr}_2[G_{0,22,k}(i\eta')G_{0,22,k-q}(-i\eta')]d^2k|_{q=0}.$$

APPENDIX C: EVALUATION OF THE MATRIX ELEMENT OF $|\Phi^0_{\pm i\eta'}\rangle$

The matrix element with respect to the average Hamiltonian $\langle H\rangle_m$ of MLG gives

$$\langle\Phi^0_{i\eta'}|r_k^2|\Phi^0_{-i\eta'}\rangle = 4(\eta'^2 + \bar{m}^2/4)\int_0^\lambda \frac{k}{(\eta'^2 + \bar{m}^2/4 + k^2)^3}\frac{dk}{2\pi}$$

$$\sim \frac{1}{2\pi(\eta'^2 + \bar{m}^2/4)}$$

for $\lambda\sim\infty$, and of BLG

$$\langle\Phi^0_{i\eta'}|r_k^2|\Phi^0_{-i\eta'}\rangle = 16(\eta'^2 + \bar{m}^2/4)\int_0^\lambda \frac{k^3}{(\eta'^2 + \bar{m}^2/4 + k^4)^3}\frac{dk}{2\pi}$$

$$\sim \frac{1}{\pi(\eta'^2 + \bar{m}^2/4)}.$$

---

[1] K. S. Novoselov, A. K. Geim, S. V. Morozov, D. Jiang, M. I. Katsnelson, I. V. Grigorieva, S. V. Dubonos, and A. A. Firsov, Nature (London) **438**, 197 (2005).

[2] Y. Zhang, Y.-W. Tan, H. L. Stormer, and P. Kim, Nature (London) **438**, 201 (2005).

[3] A. K. Geim and K. S. Novoselov, Nature Mater. **6**, 183 (2007).

[4] Y.-W. Tan, Y. Zhang, K. Bolotin, Y. Zhao, S. Adam, E. H. Hwang, S. Das Sarma, H. L. Stormer, and P. Kim, Phys. Rev. Lett. **99**, 246803 (2007).

[5] J. H. Chen, C. Jang, M. S. Fuhrer, E. D. Williams, and M. Ishigami, Nat. Phys. **4**, 377 (2008).

[6] S. V. Morozov, K. S. Novoselov, M. I. Katsnelson, F. Schedin, D. C. Elias, J. A. Jaszczak, and A. K. Geim, Phys. Rev. Lett. **100**, 016602 (2008).

[7] D. C. Elias, R. R. Nair, T. M. G. Mohiuddin, S. V. Morozov, P. Blake, M. P. Halsall, A. C. Ferrari, D. W. Boukhvalov, M. I. Katsnelson, A. K. Geim, and K. S. Novoselov, Science **323**, 610 (2009).

[8] O. Taisuke, A. Bostwick, T. Seyller, K. Horn, and E. Rotenberg, Science **313**, 951 (2006).

[9] R. V. Gorbachev, F. V. Tikhonenkoa, A. S. Mayorova, D. W. Horsella, and A. K. Savchenkoa, Physica E **40**, 1360 (2008).

[10] J. B. Oostinga, H. B. Heersche, X. Liu, A. F. Morpurgo, and L. M. K. Vandersypen, Nat. Mater. **7**, 151 (2008).

[11] E. V. Castro, N. M. R. Peres, J. M. B. Lopes dos Santos, F. Guinea, and A. H. Castro Neto, J. Phys.: Conf. Ser. **129**, 012002 (2008).

[12] V. V. Cheianov, V. I. Fal'ko, B. L. Altshuler, and I. L. Aleiner, Phys. Rev. Lett. **99**, 176801 (2007).

[13] Y.-Y. Zhang, Jiangping Hu, B. A. Bernevig, X. R. Wang, X. C. Xie, and W. M. Liu, Phys. Rev. Lett. **102**, 106401 (2009).

[14] S.-J. Xiong and Y. Xiong, Phys. Rev. B **76**, 214204 (2007).

[15] K. Ziegler, Phys. Rev. B **78**, 125401 (2008).

[16] A. W. W. Ludwig, M. P. A. Fisher, R. Shankar, and G. Grinstein, Phys. Rev. B **50**, 7526 (1994); E. Fradkin, *ibid.* **33**, 3263 (1986).

[17] K. Ziegler, Phys. Rev. B **55**, 10661 (1997); Phys. Rev. Lett. **80**, 3113 (1998).

[18] K. Ziegler, Phys. Rev. Lett. **102**, 126802 (2009).

[19] H. Suzuura and T. Ando, Phys. Rev. Lett. **89**, 266603 (2002).

[20] N. M. R. Peres, F. Guinea, and A. H. Castro Neto, Phys. Rev. B **73**, 125411 (2006).

[21] D. V. Khveshchenko, Phys. Rev. Lett. **97**, 036802 (2006).

[22] E. McCann, K. Kechedzhi, V. I. Falko, H. Suzuura, T. Ando, and B. L. Altshuler, Phys. Rev. Lett. **97**, 146805 (2006).

[23] X.-Z. Yan and C. S. Ting, Phys. Rev. Lett. **101**, 126801 (2008).

[24] M. Koshino and T. Ando, Phys. Rev. B **73**, 245403 (2006).

[25] E. McCann and V. I. Fal'ko, Phys. Rev. Lett. **96**, 086805 (2006); E. McCann, Phys. Rev. B **74**, 161403(R) (2006).

[26] S. V. Morozov, K. S. Novoselov, M. I. Katsnelson, F. Schedin, L. A. Ponomarenko, D. Jiang, and A. K. Geim, Phys. Rev. Lett. **97**, 016801 (2006).

[27] A. H. Castro Neto, F. Guinea, N. M. R. Peres, K. S. Novoselov, and A. K. Geim, Rev. Mod. Phys **81**, 109 (2009).

[28] J. C. Meyer, A. K. Geim, M. I. Katsnelson, K. S. Novoselov, T. J. Booth, and S. Roth, Nature (London) **446**, 60 (2007).

[29] P. W. Anderson, Phys. Rev. **109**, 1492 (1958).

[30] J. Cserti and G. Dávid, Phys. Rev. B **74**, 172305 (2006); M. I. Katsnelson, Eur. Phys. J. B **51**, 157 (2006); M. I. Katsnelson and K. S. Novoselov, Solid State Commun. **143**, 3 (2007); T. M. Rusin and W. Zawadzki, Phys. Rev. B **76**, 195439 (2007); U. Zülicke, J. Bolte, and R. Winkler, New J. Phys. **9**, 355 (2007); J. Schliemann, *ibid.* **10**, 043024 (2008).

[31] J. W. Negele and H. Orland, *Quantum Many-Particle Physics* (Addison-Wesley, New York, 1988).

[32] K. Ziegler, Phys. Rev. B **75**, 233407 (2007).

[33] T. Stauber, N. M. R. Peres, and A. K. Geim, Phys. Rev. B **78**, 085432 (2008).

[34] S. Adam, S. Cho, M. S. Fuhrer, and S. Das Sarma, Phys. Rev. Lett. **101**, 046404 (2008).